DOI: 10.61782/fa.2025.0626

NUMERICAL AND EXPERIMENTAL STUDY OF ACOUSTIC PERFORMANCE OF PHONONIC CRYSTALS-BASED VENTILATED NOISE BARRIERS FOR TRAFFIC NOISE

Noman Ahsan[1,2*] **Nicolas Herrera**[2] **Luca Sangiuliano**[1]
Paulo Amado Mendes[2] **Luis Godinho**[2]
[1] Phononic Vibes SRL, Via Francesco Cherubini 6, 20145, Milan, Italy
[2] University of Coimbra, ISISE, ARISE, Department of Civil Engineering, Coimbra, Portugal

ABSTRACT

Phononic crystal-based noise barriers offer promising solutions for urban noise mitigation, particularly concerning traffic and highway noise, due to their capacity to efficiently attenuate sound while maintaining ventilation. This study advances the state of the art through two key contributions: first, by developing an experimental setup to analyze stopband frequencies and, second, by creating a numerical model that replicates real-world conditions for further validation. Unlike previous studies, which primarily assessed phononic crystal barriers in semi-anechoic chambers with single noise sources, this work introduces a more realistic experimental approach. The setup utilizes an Alpha cabin with a diffuse sound field, where a 4×6 array of cylindrical scatterers is mounted on the cabin door. Insertion Loss (IL) is measured using an external microphone array, capturing the barrier's performance in practical conditions. To account for production and assembly tolerances, slight variations in the scatterers' x and y coordinates are introduced into the numerical model. Results show peak attenuation values between 1 and 2 kHz, aligning with critical urban noise frequencies. This study presents a methodology for evaluating ventilated phononic crystals in real-world scenarios, providing valuable insights for designing efficient noise barriers tailored to traffic and highway applications.

Keywords: *Acoustic Metamaterials, Phononic Crystals, Ventilated Noise Barriers, Insertion Loss, Traffic Noise*

[*] ***Corresponding author***: *noman.ahsan@phononicvibes.com*

1. INTRODUCTION

Noise pollution is a growing concern in urban environments, impacting public health and well-being. Prolonged exposure to excessive noise levels can result in hearing loss, cardiovascular issues, sleep disturbances, and cognitive impairments, particularly in children. Conventional noise barriers, while effective in reducing sound transmission, tend to be bulky and visually intrusive, blocking natural airflow. These limitations have spurred the search for alternative solutions, with phononic crystal-based noise barriers emerging as a promising innovation.

Phononic crystals (PCs), a type of acoustic metamaterial, utilize periodic structures to control wave propagation, providing enhanced noise reduction while still allowing for ventilation. Recent studies have explored their ability to reduce traffic noise, but practical applications remain limited. PCs can create stopbands, which are frequency ranges where sound transmission is blocked, making them particularly effective for targeted noise reduction. However, further research is necessary to optimize their design for real-world applications.

Traffic noise is one of the primary sources of urban noise pollution, affecting large populations in cities due to the high volume of vehicles and continuous road traffic. Figure 1 illustrates the spectral energy contribution rate of traffic noise at various vehicle speeds, ranging from approximately 34 km/h to 93 km/h. Figure 2 displays the sound pressure levels (SPL), in dB(A), at ground level as a function of frequency. Both figures emphasize that traffic noise is most prominent between 500 Hz and 2 kHz, with a peak between 1 kHz and 1.6 kHz. This observation aligns with typical noise sources, including engine vibrations, tire-road interactions, and aerodynamic effects. The energy distribution increases significantly within this frequency range, indicating that any effective noise mitigation strategy must focus on these frequency bands.

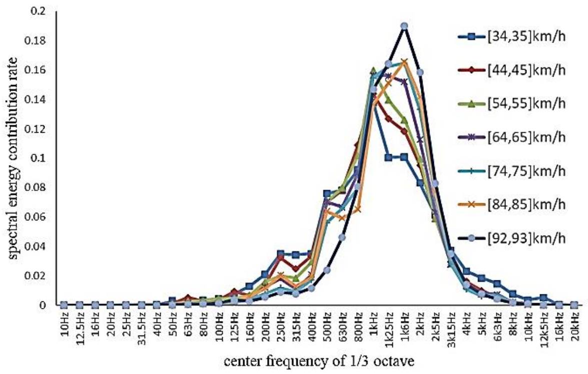

Figure 1. Traffic Noise Spectrum showing dominant frequencies [1]

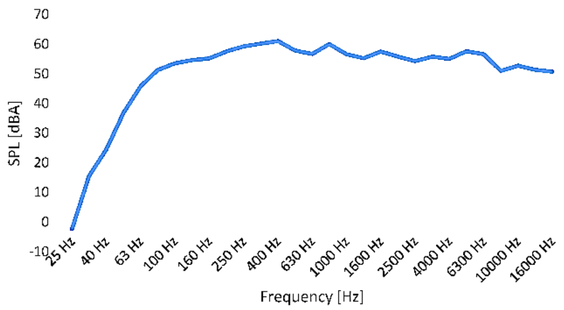

Figure 2. SPL versus frequency recorded in traffic-generated noise measurements [2]

In recent years, acoustic metamaterials have been increasingly utilized to mitigate traffic noise, capitalizing on their unique ability to manipulate sound waves. Sonic crystals and phononic crystals have garnered attention for their ability to control sound propagation, especially at frequencies where traffic noise is typically present. Sonic crystals use periodic arrays of scatterers to create band gaps that block specific frequencies of sound [3]. Phononic crystals, on the other hand, utilize periodic structures at the scale of acoustic wavelengths to prevent the transmission of sound, making them highly effective for controlling low-frequency noise [4]. Their tunable properties enable the precise targeting of problematic noise frequencies, making them highly adaptable for various applications in traffic noise control.

This study presents an integrated approach that combines numerical modeling with experimental validation to evaluate the performance of an array of phononic crystal-based noise barriers. A 4×6 array of cylindrical scatterers was tested in a diffuse sound field within an Alpha cabin, with Insertion Loss (IL) measurements taken externally. By incorporating production tolerances into numerical analysis, this research provides a more realistic evaluation of PC barriers. The findings demonstrate peak attenuation between 1 and 2 kHz, which aligns with the dominant frequencies of urban noise pollution. This work contributes to the advancement of sustainable, high-performance noise control solutions suitable for traffic and highway applications.

2. THEORY AND DESIGN

Phononic crystals (PCs) are artificially engineered periodic structures that manipulate the propagation of elastic and acoustic waves. These structures achieve sound attenuation by introducing bandgap frequency ranges where wave transmission is significantly suppressed. The attenuation mechanism primarily relies on Bragg scattering and local resonance effects [5].

The concept of sonic crystals was first introduced by Martinez [6] in 1995. They conducted sound attenuation experiments on a sculpture by Eusebio Sempere, which was displayed at the Juan March Foundation in Madrid. The team measured sound attenuation under outdoor conditions, focusing on sound wave vectors that were aligned perpendicularly to the vertical axis of the cylinder. They identified a sound attenuation peak at 1670 Hz, marking the emergence of the first band gap.

Figure 3: Different types of Sonic Crystals, also known as periodic structures

According to Bragg's law [7], the mechanism of sound attenuation involves the destructive interference of reflected sound waves with incident sound waves within the band gaps. If the interference is constructive, then the energy of the original wave gets transmitted through the sonic crystal, which forms the propagation bands. In Bragg scattering, destructive interference occurs when the wavelength of an incident wave matches the periodicity of the structure. The Bragg condition for a 1D periodic structure is given by:

$$m\lambda = 2d\sin\theta \qquad (1)$$

Where m is the diffraction order (usually m = 1 for the first Bragg condition), λ is the wavelength of the incident wave, d is the lattice constant (the periodic spacing of the scatterers), θ is the angle of incidence of the wave relative to the structure. For a 2D phononic crystal, where periodicity is in two dimensions, the formation of a stopband is governed by the Bloch wave condition using the dispersion relation:

$$k = k0 + G \qquad (2)$$

Where k is the wavevector in the phononic crystal, k_0 is the incident wavevector, and G is the reciprocal lattice vector. This equation describes the multiple scattering effect, where waves interfere constructively and destructively, leading to bandgap formation [8]. For periodic scatterers with a lattice constant a, the Bragg Bandgap frequency can be approximated as:

$$f_b = \frac{c}{2a} \qquad (3)$$

Where c is the speed of sound in the background medium, this relation shows that the stopband shifts to lower frequencies as the lattice spacing increases, making it a crucial design parameter in phononic crystal barriers. In theory, band gaps should be at multiples of the above fundamental frequency.

Similarly, the filling fraction, a crucial property, influences the width of the band gap. It indicates the proportion of the structure filled by the cylinders [4]. For a square lattice arrangement with scatterers of radius r, the filling fraction is defined as

$$F = \frac{\pi r^2}{a^2} \qquad (4)$$

The fundamental component of a phononic crystal is its unit cell, which can be a scatterer or multiple scatterers and can have shapes such as cylindrical, square, or spherical, organized in a periodic pattern. The selection of lattice configuration, whether square, hexagonal, or triangular, greatly influences wave propagation characteristics. A square lattice featuring cylindrical scatterers is frequently used in phononic crystal barriers due to its simplicity in production and the reliable creation of bandgaps.

In this study, we have modeled and tested a unit cell with a lattice constant of 15 cm, a scatterer diameter of 10 cm, and a height of 100 cm to investigate the effectiveness of sonic crystal-based noise barriers in attenuating traffic noise. Figure 4 illustrates the dimensions and geometry of a single unit cell. For the array configuration, we opted for four rows and six columns of scatterers, which was determined to provide an optimal trade-off between acoustic performance and structural efficiency. This array configuration ensures sufficient coverage of the target frequencies while minimizing material usage and production complexity.

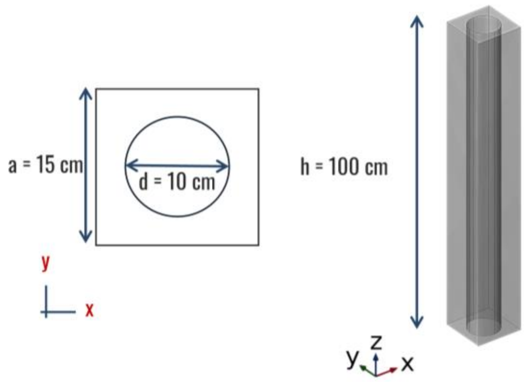

Figure 4: Unit Cell representing one barrier with a=lattice constant, d=diameter of scatterer, and h=height of scatterer

Using the designed unit cell, a numerical model was developed in COMSOL Multiphysics, complemented by an experimental setup, to study the acoustic performance of the unit cell and the array of barriers. The numerical simulations allowed for a detailed analysis of sound wave interactions with the scatterers, while the experimental setup provided empirical data for validation. This methodology enabled a comprehensive evaluation of the noise attenuation capabilities of the barriers, as detailed in Section 4, and the results are discussed in Section 5.

3. METHODOLOGY

3.1 Stopband Analysis

An eigenfrequency study is conducted on the unit cell shown in Figure 6 to determine its band structure and eigenmodes by analyzing the first five eigenfrequencies. A parametric sweep is performed for the wave vector kx along the wave propagation direction over the range $0 \leq kx \leq \pi/a$, which corresponds to the irreducible part of the Brillouin zone.

This analysis helps identify phononic bandgap frequency ranges where wave propagation is prohibited by observing gaps in the computed eigenfrequencies. The resulting dispersion curve provides insights into the wave propagation characteristics of the phononic crystal, enabling the optimization of its design for effective noise attenuation, particularly within the 500 Hz–2 kHz range, which is relevant to traffic noise.

3.2 Numerical Model

To evaluate the acoustic performance of a periodic sonic crystal array in a realistic setting, a comprehensive 3D finite element model was developed using COMSOL Multiphysics. The simulation focused on predicting the insertion loss (IL) and identifying the acoustic stopband behavior of a 4 × 6 array of scatterers, tailored to replicate a real-world prototype under diffuse field conditions. A conceptual diagram is illustrated in Figure 5.

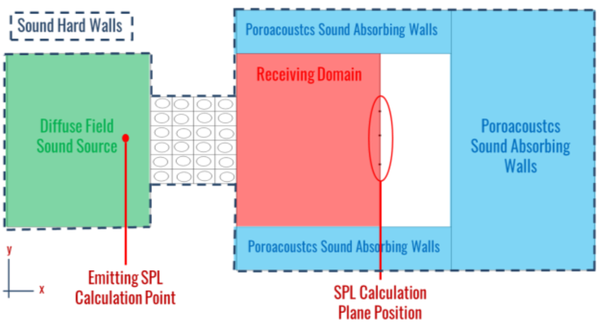

Figure 5: 2D Graphical representation of numerical model used in COMSOL to compute Insertion Loss

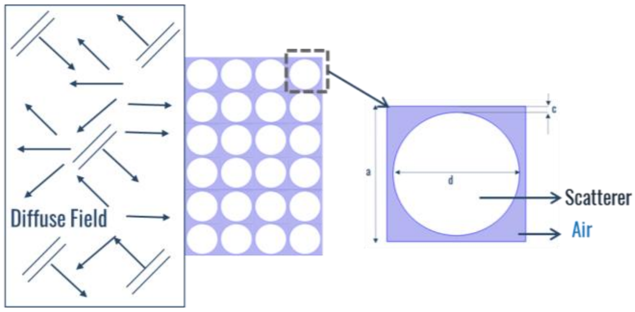

Figure 6: Air applied on surrounding domain of scatterer and random pressure in emitting domain

Table 1. Geometric Parameters of Unit Cell.

Parameter	Description	Value
a	Lattice Constant	15 cm
d	Diameter	10 cm
c	Gap	5 cm

The simulated geometry represents a 3D array of 24 cylindrical scatterers (4 rows × 6 columns) positioned in air, as illustrated in Figures 5 and 6. Scatterers are infinitely rigid and, on the source side, random pressure input diffuse field effects.

In the absence of flow and thermal effects, the Helmholtz equation governs the acoustic pressure field in the frequency domain:

$$\nabla \cdot \left(\frac{1}{\rho_0} \nabla p \right) + \frac{\omega^2}{\rho_0 c_0^2} p = 0 \qquad (6)$$

where:

- p is the complex acoustic pressure [Pa],
- ρ_0 is the air density [kg/m^3],
- c_0 is the speed of sound in air [m/s],
- $\omega = 2\pi f$ is the angular frequency [rad/s].

To replicate realistic boundary absorption (instead of using perfectly matched layers, PML), porous absorbing materials were modeled using the Johnson-Champoux-Allard (JCA) framework, valid for rigid-frame porous media. To replicate environmental excitation such as traffic noise, a diffuse acoustic field was approximated numerically by summing multiple incident plane waves over an emitting domain. This mimics a random incidence angle distribution:

$$p_{\text{inc.}}(\mathbf{r}) = \sum_{\pi\downarrow}^{N} A_n e^{-j\mathbf{k}_n \cdot \mathbf{r}} \quad (8)$$

where:

- r: position vector,
- k_n: incident wave vector for angle θ_n and ϕ_n
- A_n: complex amplitude (random phase),
- N: number of plane waves.

Considering geometric variations for realism, this model simulates prototype inaccuracies and production tolerances, precisely scatterer position offsets.

Insertion Loss (IL) measures the reduction in sound transmission that occurs when a barrier is inserted into the acoustic path. In the model, IL is calculated as the difference in Transmission Loss (TL) between the reference case (an empty domain) and the case with the present barrier. Sound pressure levels (SPL) were measured inside and outside the array, and the IL of the variety was computed in dB using TL with and without barriers as explained in the following relations:

$$TL_{empty} = SPL_{inside} - SPL_{outside}$$

$$TL_{barriers} = SPL_{inside} - SPL_{outside}$$

$$IL\ (dB) = TL_{barriers} - TL_{empty}$$

$$= SPL_{outside\ (Empty)} - SPL_{outside\ (Barriers)}$$

The difference in TL values isolates the acoustic effect of the barrier, effectively accounting for diffraction and scattering. This method ensures a reliable and realistic evaluation of the barrier's performance, consistent with established acoustic standards.

3.3 Experimental Setup

To experimentally validate the stop-band effect of the sonic crystal array due to Bragg scattering, measurements were conducted by installing a sonic crystal (SC) array on the door of an Alpha Cabin reverberant cabin, which serves as a diffuse-field sound source. Sound excitation was generated using six high-power loudspeakers capable of producing a sound power of up to 115 dB, thereby creating a diffuse sound field that simulates real-world noise conditions, as shown in Figures 7 and 8.

A 4×6 array of rigid PVC pipes, acting as sonic crystals, was installed on the door of the measurement cabin. Each scatterer has a diameter of 10 cm and is arranged in a square lattice with a 15 cm periodicity, resulting in an array with a width of 90 cm, a depth of 60 cm, and a height of 100 cm.

The pipes were filled to avoid any resonances and precisely arranged to maintain the desired periodicity required for Bragg scattering. To prevent unwanted sound leakage, the array was fully sealed with wooden panels on all four sides- top, bottom, left, and right- except for the side facing the microphone array.

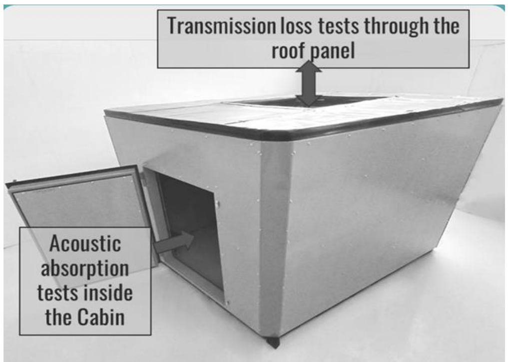

Figure 7: Phononic Vibes 9m^3 Alpha Cabin

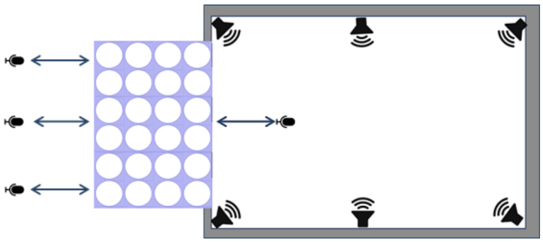

Figure 8: Schematics showing how source and receiving domain look in experimental setup

This configuration ensures that sound waves existing in the cabin must pass through the periodic structure, facilitating selective frequency attenuation via the bandgap effect.

A 2D array of seven microphones is positioned 60 cm from the last row of the SC array to capture transmitted sound levels. To accurately capture sound pressure levels (SPL), seven microphones were placed in front of the array, and one microphone was positioned inside the cabin. This multi-point measurement approach enabled spatial logarithmic averaging, reducing position-dependent variations and providing a more representative assessment of the overall sound attenuation caused by the barrier.

Table 2. Description of Microphones and their distances.

Microphone no.	Position	Distance from Array
Mic1	Receiving	60 cm
Mic2	Receiving	60 cm
Mic3	Receiving	60 cm
Mic4	Receiving	60 cm
Mic5	Receiving	60 cm
Mic6	Receiving	60 cm
Mic7	Receiving	60 cm
Mic8	Emitting	60 cm

Sound pressure levels (SPL) were measured at multiple positions inside and outside the phononic crystal array to evaluate its noise attenuation performance. The microphone-facing walls of the Alpha cabin were covered with sound-absorbing material to minimize unwanted reflections and prevent any unnecessary resonances that could interfere with the accuracy of the measurements. Additionally, the wall behind the microphone array was also treated with absorbent material to eliminate back reflections, ensuring that the recorded sound levels accurately represent the transmitted sound without contamination from secondary reflections, as shown in Figures 9 and 10.

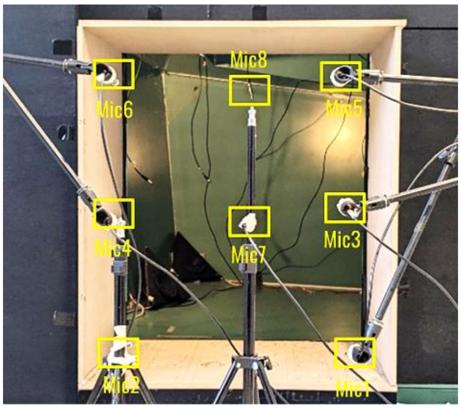

Figure 9: Baseline: No barriers installed and SPL_{empty} measured inside (Mic8) and outside (Mic1-7) to computed TL_{empty}

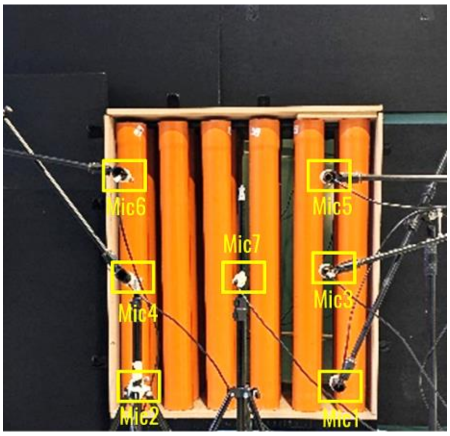

Figure 10: Barriers installed and $SPL_{barriers}$ measured inside (Mic8) and outside (Mic1-7) to computed $TL_{barriers}$

Given the periodic arrangement of the SC array, Bragg scattering effects are expected to cause significant attenuation in the 500–2 kHz range, which corresponds to the dominant frequencies of traffic noise. The measured IL data will validate the formation of a bandgap and assess the overall effectiveness of the SC array in noise mitigation applications.

4. RESULTS AND DISCUSSION

The numerical and experimental results indicate that the phononic crystal (PC) array exhibits strong attenuation characteristics within the designed frequency range. The dispersion analysis of the unit cell (Figure 11) confirms the presence of a complete stopband between 1300 Hz and 1400 Hz, demonstrating the periodic arrangement's potential to suppress wave propagation effectively. This range aligns well with the observed peak insertion loss (IL) in the numerical simulations (Figure 13).

Figure 13 illustrates the insertion loss obtained for the 4x6 array of scatterers, comparing the ideal periodic arrangement with a structure incorporating random variations in scatterer positioning along the x- and y-coordinates. The results show that the perfectly periodic PC configuration achieves a maximum IL of approximately 16 dB at 1250 Hz, validating its effectiveness in mitigating noise in the mid-to-high-frequency range, with a grey-shaded envelope representing the range between maximum and minimum values.

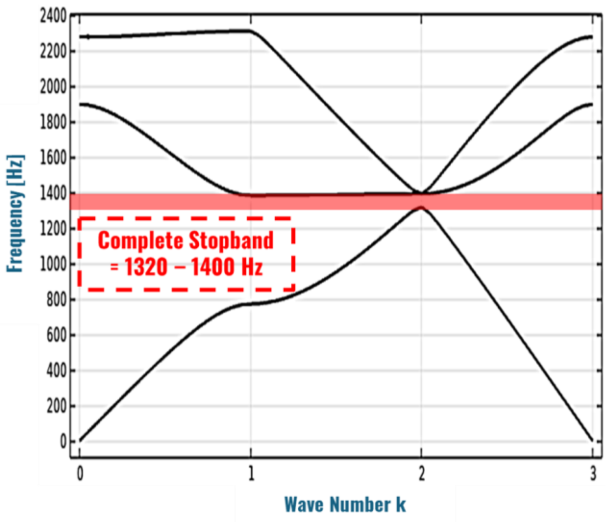

Figure 11: Dispersion Curve showing a complete stop band of designed unit cell between 1300-1400 Hz

The application of random variation along scatterers introduces some fluctuation in the insertion loss response yet maintains a strong attenuation band centered around 1250 Hz. The broadening of the attenuation peak suggests improved robustness and potential for practical deployment, where production imperfections and environmental conditions would otherwise degrade performance.

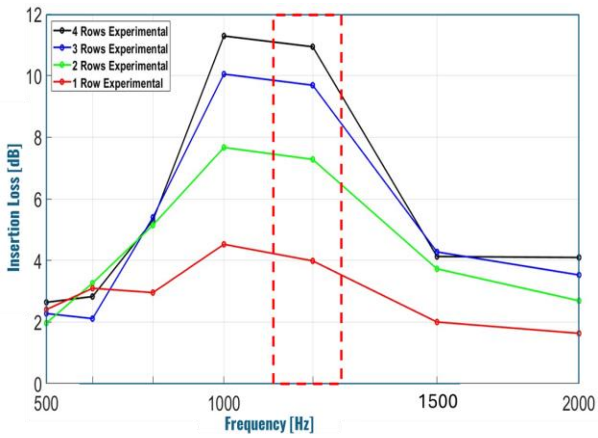

Figure 12: Experimentally measured IL showing the stopband between 1000-1500 Hz in 1/3 Octave bands

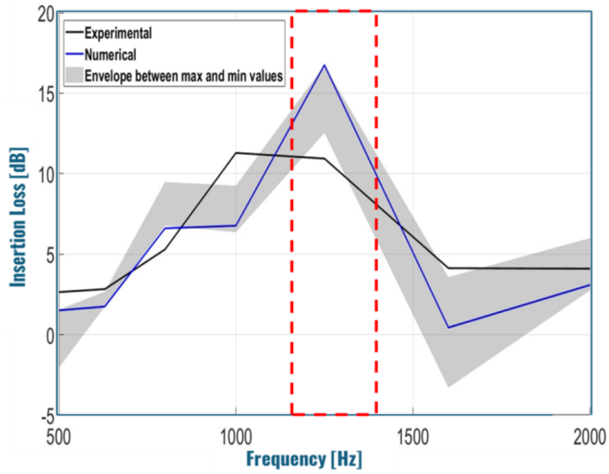

Figure 13: Experimental vs Numerical IL of 4x6 Array of Barriers

Figure 12 shows the experimentally computed IL with different numbers of rows of the barriers. The incremental increase in IL with additional rows suggests that multiple scattering and destructive interference significantly contribute to noise reduction. The experimental results demonstrate the effectiveness of the sonic crystal noise barrier in reducing sound transmission, particularly in the 1000–1400 Hz range, where the insertion loss (IL) reaches a peak of approximately 12 dB for the 4-row configuration.

Figure 13 shows a comparison between experimental and numerical IL for a 4x6 array of barriers, considering variation, and confirms the presence of a stopband between the desired frequencies. The deviations between experimental and numerical data could stem from imperfect boundary conditions (such as wooden panels), production tolerances, or edge diffraction effects.

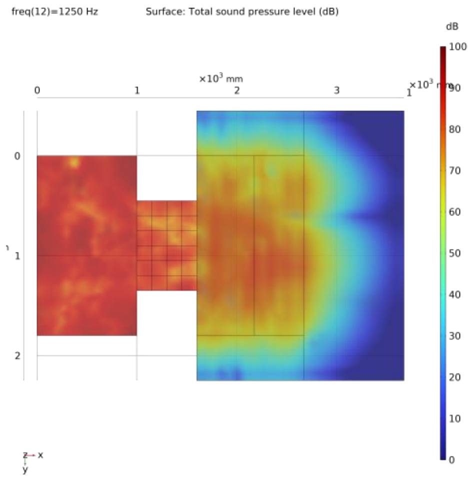

Figure 14: With no barriers, no apparent reduction in SPL

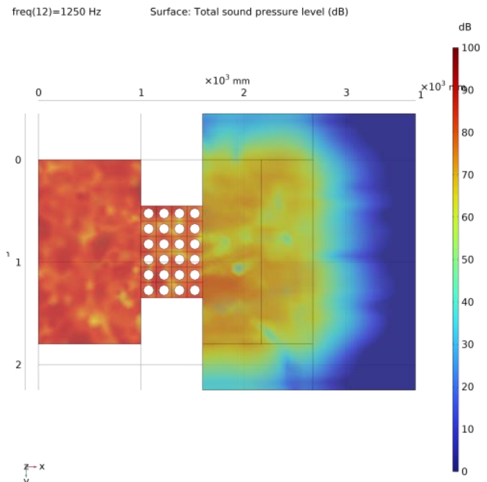

Figure 15: SPL reduced in receiving domain with barriers

Figure 14 shows the scenario without barriers, where SPL remains high and widespread, indicating minimal noise reduction. In contrast, Figure 15 presents the sound pressure level (SPL) distribution, demonstrating reduced SPL in the receiving domain when barriers are present, confirming their noise mitigation capability. These results highlight the effectiveness of the barrier array in controlling noise propagation within stopband frequencies.

5. ACKNOWLEDGMENTS

We gratefully acknowledge the European Commission for its support of the Marie Sklodowska Curie program through the Horizon Europe DN METAVISION project (GA 101072415).

This work was partly financed by FCT / MCTES through national funds (PIDDAC) under the R&D Unit Institute for Sustainability and Innovation in Structural Engineering (ISISE), under reference UID/04029/Institute for Sustainability and Innovation in Structural Engineering (ISISE), and under the Associate Laboratory Advanced Production and Intelligent Systems ARISE under reference LA/P/0112/2020.

6. REFERENCES

[1] Yang, Weijun, Ming Cai, and Peng Luo. "The calculation of road traffic noise spectrum based on the noise spectral characteristics of single vehicles." Applied Acoustics 160 (2020): 107128.

[2] Minea, Marius, and Cătălin Marian Dumitrescu. "Urban traffic noise analysis using uav-based array of microphones." *Sensors* 23.4 (2023): 1912.

[3] Chen, Qiqi, et al. "Review of Phononic crystals and acoustic metamaterials." *IOP Conference Series: Materials Science and Engineering*. Vol. 788. No. 1. IOP Publishing, 2020.

[4] Liu, Xiaohua, et al. "Pneumatic soft phononic crystals with tunable band gap." *International Journal of Mechanical Sciences* 240 (2023): 107906.

[5] Bragg WH, Bragg WL (1913) The reflexion of X-rays by crystals. Proc R Soc Lond A 88(605):428–438

[6] Martínez-Sala, Rosa, et al. "Sound attenuation by sculpture." nature 378.6554 (1995): 241.

[7] Page, John H., et al. "Phononic crystals." *physica status solidi (b)* 241.15 (2004): 3454-3462.

[8] Kittel C (1996) Introduction to solid state physics. Wiley, New York